Velocity selective optical pumping and dark resonances in selective reflection spectroscopy

B. Gross, N. Papageorgiou,[*] V. Sautenkov,[†] and A. Weis[‡]

Max-Planck-Institut für Quantenoptik, Hans-Kopfermann-Strasse 1, 85748 Garching, Germany

(Received 20 September 1996)

We report an experimental investigation of selective reflection spectra using a bichromatic field with a resonant Λ-type coupling to the D_1 transition of Rb vapor atoms. The reflection spectra are found to have a more complex structure than equivalent spectra in transmission experiments. This structure is traced back to the effect of wall collisions on velocity selective optical pumping and saturation processes. The spectral line shapes are well described by a theoretical model developed in the text. In addition we report the observation of dark resonances in reflection spectroscopy. [S1050-2947(97)00104-2]

PACS number(s): 32.80.Bx, 34.50.Dy, 32.70.Jz, 42.25.Gy

I. INTRODUCTION

The technique of selective reflection (SR) spectroscopy consists of monitoring the spectral dependence of the reflection coefficient $R(\omega)$ of the interface between a transparent dielectric and an atomic vapor [1–3]. The origin of the resonant variation of the reflected light intensity is the constructive interference between the Fresnel reflected field from the interface and the field emitted by vapor atoms within a distance of the order of the optical wavelength from the surface. As a result the SR spectrum contains information about the properties of neutral atoms near the dielectric surface and hence may be used to study properties of optically thick media, atom-surface collisions, long-range atom-surface interactions, or QED effects near the interface [4]. Another prominent feature of SR spectra is that they yield, even in a linear regime, resonances with sub-Doppler widths.

Linear SR spectroscopy, among other techniques, has been used in the past to measure the collision-induced broadening and shift of atomic resonance lines [5–7], the van der Waals attraction between Cs atoms and a dielectric surface [8,9], the Zeeman structure of the Cs D_2 line in intermediate magnetic fields [10], magnetic level crossing resonances in the excited [11,12] and in the ground state [13], magnetorotation, and magnetic circular dichroism [14].

A theoretical study of the saturation behavior of SR from a diluted gas of two level atoms was performed by Vartanyan [15]. Nonlinear SR from three-level atoms under bichromatic excitation in the cascade or Λ configuration was theoretically studied in [17,18] and various experiments using two monochromatic beams in pump-probe schemes were reported [19]. Recently a bichromatic pump-probe experiment in SR has been reported for a cascade system [20]. The latter work confirmed theoretical calculations and discussed the possibility to apply the technique to probe atomic velocity distributions near the surface.

The present work describes an experimental investigation of reflection spectra from an atomic vapor using a bichromatic pump-probe scheme in which the optical fields are coupled in a Λ configuration to resonant atomic transitions. The main objective of these experiments was the study of dark states, i.e., coherent superpositions of the lower atomic states which are decoupled from the light fields. A theoretical model describing the properties of such states in three-level atoms was recently published [18]. For our study we chose the hyperfine components $5S_{1/2}(F=2) \rightarrow 5P_{1/2}(F'=2,3)$ and $5S_{1/2}(F=3) \rightarrow 5P_{1/2}(F'=2,3)$ of the D_1 transition of ^{85}Rb, which are easily accessed with diode lasers. Alkali-metal atoms have a complex multilevel structure and the observation of coherent effects is overshadowed by incoherent processes such as velocity selective optical pumping and/or collisional population redistribution. In order to discriminate the dark resonances properly against these incoherent background processes we performed an extensive study of the latter. As the coherent processes are most pronounced when the two optical fields are of comparable intensity the incoherent processes can be isolated by the use of a pump-(strong field) probe (weak field) technique.

This paper is organized as follows: We first revise the basic features of linear SR spectroscopy of two-level atoms (Sec. II). In Sec. III we study the incoherent processes occurring in SR with bichromatic excitation. We develop a simple theoretical model and compare its predictions with experimental results. In Sec. IV we describe the theoretical and experimental studies of dark resonances in SR.

II. SELECTIVE REFLECTION FROM TWO-LEVEL ATOMS

Consider a monochromatic plane wave of frequency ω at normal incidence on the interface between a transparent dielectric and a dilute atomic vapor composed of two-level atoms with resonance frequency ω_{bc}. The optical field entering the vapor induces a position- and velocity-dependent atomic polarization $p(z,v_z)$, and the resonant variation of the reflection coefficient $SR(\omega-\omega_{bc})$ is obtained [24] by integrating this polarization over the distance from the surface z (the atomic vapor fills the $z>0$ half space) and over all atomic velocity classes v_z,

*Present address: Université de Provence, CIIM Case C21, St. Jerôme, F-13397 Marseille, France.

†Present address: Huygens Laboratorium, Leiden University, P.O. Box 9504, 2300 RA Leiden, The Netherlands.

‡Present address: Institut für Angewandte Physik, Universität Bonn, Wegelerstr. 8, 53115 Bonn, Germany.

$$SR(\omega - \omega_{bc}) \propto \int_0^\infty dz e^{2ikz} \int_{-\infty}^{+\infty} dv_z \underbrace{W(v_z)\mathrm{Re}\rho_{bc}}_{p(z,v_z)}.$$

$$(1)$$

Here ρ_{bc} is the off-diagonal matrix element of the atomic density matrix and

$$W(v_z)dv_z = (u\sqrt{\pi})^{-1}e^{-v_z^2/u^2}dv_z$$

is the Maxwellian velocity distribution of the atoms with $u = \sqrt{2kT/m}$ being the most probable thermal velocity.

The SR spectrum at near-normal incidence is a Doppler-broadened dispersive curve featuring a sharp sub-Doppler singularity around the atomic resonance frequency ω_{bc} [3]. The origin of this singularity is the transient behavior of atoms leaving the interface. Atoms moving towards the interface ($v_z < 0$) are embedded for a long time in the transmitted optical field and are in a steady state regime of interaction with it. Conversely, atoms leaving the interface ($v_z > 0$) have suffered a quenching of their dipole optical excitation when colliding with the dielectric surface. Despite this asymmetry one can show that for low light intensities the contribution of incoming and outgoing atoms to the SR signal are identical [25].

In the linear regime, i.e., when ignoring saturation, the integration over z may be carried out explicitly and the SR profile, in the Doppler limit (Doppler width, $ku \gg$ homogeneous width, γ) is given by

$$SR(\omega) \propto 2\int_{-\infty}^0 dv_z W(v_z)\mathrm{Re}\frac{1}{\Delta_{bc}(\omega, v_z)}, \qquad (2)$$

where we have used the steady-state solution $\rho_{bc}^{-1} \propto \Delta_{bc}$. The complex frequency detuning from the Doppler shifted atomic resonance frequency is given by $\Delta_{bc}(\omega, v_z) = \omega - \omega_{bc} - kv_z + i\gamma/2$, where γ is the homogeneous width of the transition. Note that it is the integration over a truncated velocity space that leads to the peculiar sub-Doppler line shapes encountered in SR spectra. Due to the destructive interference of the light emitted by the atoms from the homogeneous volume in the backward direction the main contribution to the reflection signal is due only to atoms within a thin layer near the interface of thickness $\sim\lambda/2\pi$.

Equation (2) is the basis for the theoretical calculations performed below, in which we consider changes induced by the presence of a second light field that modifies the atomic velocity distribution and/or the optical coherence ρ_{bc}.

III. INCOHERENT EFFECTS IN SELECTIVE REFLECTION SPECTRA FROM A THREE-LEVEL Λ SYSTEM

A. Theory

In this section we investigate the incoherent modifications on the SR spectrum of a weak probe beam induced by a strong pump beam that produces saturation and velocity selective optical pumping (VSOP). Let the vapor be composed of three-level atoms with ground states a and c and an excited state b (Fig. 1). We suppose that the frequency splitting
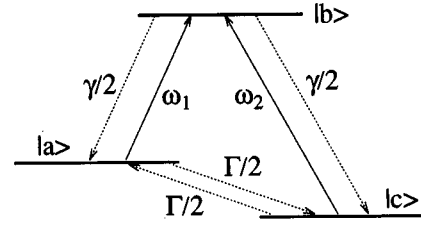

FIG. 1. Three-level Λ system. In the text light fields 1 and 2 are referred to as pump and probe field.

of the two ground states a and c is large enough so the pump lasers with frequency ω_1 interacts only with the $a \to b$ transition and the probe laser with frequency ω_2 interacts only with the $c \to b$ transition. The light field 1 (pump laser) is supposed to be much stronger than the field 2 (probe laser). In this system optical pumping can occur by means of population transfer from state a to state c via state b. This transfer is effective only for atoms that are Doppler shifted into resonance by $\omega_{ab} = \omega_1 - k_1 v_z$. As a result, optical pumping modifies the velocity distributions of the populations of both ground-state levels. A dip appears in the atomic velocity distribution $W_a(v_z)$ of atoms in state a around the velocity class v_z, and corresponding peaks (inverted dips) appear on the velocity distributions of atoms in states c and b. This is the well-known phenomenon of hole burning. If we neglect saturation of the transition $a \to b$ the velocity distribution of the excited state is not modified and the velocity distribution $W_c'(v_z)$ of the atomic populations in the level c is described by

$$W_c'(v_z) = (1+L)W_c(v_z), \qquad (3)$$

where $L = L(\omega_1, v_z)$ is the line shape of the inverted dip in state a.

We consider that the population in the excited state b can decay into either one of the ground states a or c with equal decay rates $\gamma/2$. In addition we consider a nonradiative relaxation rate Γ between the populations of the two ground states. At moderate atomic densities, where interatomic collisions do not induce hyperfine transitions, this relaxation rate is due to the finite interaction time of the atoms with the light field (time-of-flight relaxation). We write the following rate equations for the three populations:

$$\dot{\rho}_{aa} = \gamma_p(\rho_{bb} - \rho_{aa}) + \frac{\gamma}{2}\rho_{bb} - \frac{\Gamma}{2}(\rho_{aa} - \rho_{cc}),$$

$$\dot{\rho}_{bb} = -\gamma_p(\rho_{bb} - \rho_{aa}) - \gamma\rho_{bb},$$

$$\dot{\rho}_{cc} = \frac{\gamma}{2}\rho_{bb} + \frac{\Gamma}{2}(\rho_{aa} - \rho_{cc}), \qquad (4)$$

where γ_p is the excitation pump rate, which, for a two-level system, is given by

$$\gamma_p(\delta_1) = \frac{2\Omega_1^2}{\gamma}\frac{1}{1 + (2\delta_1/\gamma)^2},$$

where $\delta_1 = \omega_1 - \omega_{ab} - k_1 v_z$ is the detuning and $\Omega_1 = \boldsymbol{\mu}_{ab} \cdot \mathbf{E}/\hbar$ is the Rabi frequency of the pump beam with $\boldsymbol{\mu}_{ab}$ the electric dipole moment of the optical transition

$a \rightarrow b$. In the limit $\Gamma \ll \gamma, \Omega_1 \ll \gamma$ (no saturation) all atoms interacting resonantly with the optical field are pumped into the nonresonant state c and the steady-state value of the excited state population is $\rho_{bb} \rightarrow 0$. The steady-state solution for the population ρ_{cc} is then

$$\rho_{cc} = \frac{1}{2}\left(1 + \underbrace{\frac{\gamma^2}{4}\frac{S_{\text{op}}}{\delta_1^2 + (\gamma^2/4)(1+S_{\text{op}})}}_{L(\omega_1, v_z)}\right) \quad (5)$$

$L(\omega_1, v_z)$ describes the excess of population in state c. This dip has a power-broadened width (full width at half maximum) of $\Delta\omega = \gamma\sqrt{1+S_{\text{op}}}$, where

$$S_{\text{op}} = 2\frac{\Omega_1^2}{\gamma\Gamma} = \frac{\gamma_p(0)}{2\Gamma}$$

is the optical pumping saturation parameter. Note that in the limit $\Gamma \ll \Omega_1 \ll \gamma$ the optical pumping process $a \rightarrow c$ may be completely saturated without saturating the $a \rightarrow b$ transition for which the optical saturation parameter is Ω_1^2/γ^2.

The former result [Eq. (5)] can be applied directly to describe transmission experiments in which a weak probe beam is used to detect the population changes induced by the pump beam. As all atomic dipoles are in the steady-state regime of the atom-field interaction, the calculation of the probe absorption is straightforward. In the case of reflection spectroscopy, however, the transient regime of atoms departing from the surface deserves special attention. We recall that only atoms within a layer of thickness of the reduced optical wavelength ($\lambda/2\pi$) contribute significantly to the SR signal. Atoms with negative velocities (moving towards the surface) are embedded long enough in the transmitted field so that they reach their steady-state regime of optical pumping. Outgoing atoms with $v_z > 0$ have suffered a collision with the dielectric surface, which has quenched the optical dipole and has partly or fully rethermalized the ground state populations. After departing from the interface these atoms have to readjust their dipole oscillation to the laser excitation. Atoms leaving the surface do not reach steady state while traversing the layer of thickness $\lambda/2\pi$. Moreover, no significant optical pumping takes place, as can be seen from the following argument. On resonance the pump laser interacts with atoms in a velocity class of spread $\Delta v \approx \gamma/k_1$ centered around $v = 0$ which, on average, spend a time $t = \lambda/2\pi\Delta v = 1/\gamma$ in the surface layer. For atoms with $v \gtrsim \gamma/k_1$ this time is even shorter. The time required for one pumping cycle a to c is limited by the population transfer rate from a to b in a non-saturating regime and by the population decay rate γ of the excited state b in a strong saturation regime. In the first case ($\gamma_p \ll \gamma$) the total number of pumping cycles experienced by an atom before leaving the surface layer is given by $N_P = \gamma_p/\gamma \ll 1$. For a strongly saturating laser intensity ($\gamma_p \gg \gamma$) one has $N_p \approx 1$. The number of pumping cycles is further reduced for large detunings. In multilevel atoms (the particular case treated below has a ground state with 12 Zeeman sublevels) many pumping cycles are needed in order to substantially affect the medium susceptibility.
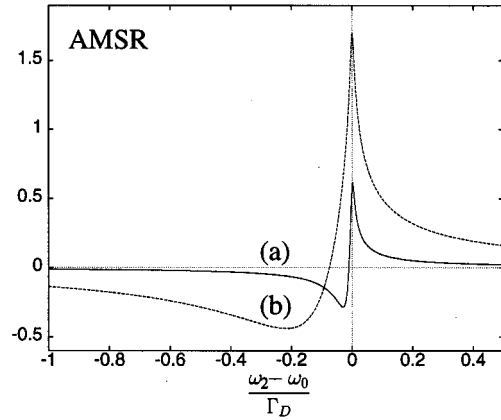

FIG. 2. Calculated AMSR signal Eq. (6) for a resonant pump laser ($\omega_1 - \omega_{ab} = 0$) for two different values of the saturation parameter: $S_{\text{op}} = 10$ (a) and $S_{\text{op}} = 100$ (b).

As a consequence VSOP is not efficient for departing atoms and one can totally neglect the contributions of departing atoms to the VSOP signal. This hypothesis was recently confirmed by a detailed numerical calculation of the transient response of departing atoms in a theoretical study of bichromatic SR from a three-level Λ system [18]. The results of that work showed indeed that contributions from departing atoms to the VSOP signal are negligible for large detunings.

Neglecting VSOP for departing atoms considerably simplifies the theoretical modeling as transient effects do not have to be taken into account. In our experiments we isolate signal contributions induced by the pump beam by amplitude modulating the latter (100% modulation) and recording the in-phase changes of the reflected probe beam intensity. We call this signal amplitude modulated selective reflection (AMSR). If we assume an instantaneous response of the system (modulation frequency $\ll$ optical pumping rate) the theoretical AMSR signal is given by the difference of the probe beam SR profiles calculated with and without the presence of the pump beam:

$$I_{\text{AMSR}}(\omega_1, \omega_2) \propto \int_{-\infty}^{0} dv_z L(\omega_1, v_z) W_c(v_z) \text{Re}\frac{1}{\Delta_{bc}(\omega_2, v_z)}. \quad (6)$$

The subtraction results in a Doppler-free VSOP signal around the pumped velocity class. The calculated line shapes of these signals for a resonant pump frequency ($\omega_1 - \omega_{ab} = 0$) and for a red detuned pump frequency with ($\omega_1 - \omega_{ab} = -0.5k_1u$) are shown in Figs. 2 and 3 for different pump laser intensities. We have used $\gamma/k_1u = 0.01$ and $\Gamma/k_1u \approx 0.001$ for all calculations. The latter reflects the transit time broadening of a Rb atom flying through a light beam of a few millimeters. In the case of a resonant pump field the line shape of the signal is an asymmetric, power broadened dispersion, which has narrow maximum on resonance. For an off-resonant pump frequency the VSOP signal is a symmetric dispersively shaped resonance centered on the pumped velocity class $k_1v = -0.5k_1u$ for low intensities. At higher intensities this resonance is power broadened and slightly blueshifted. In addition, a second, absorptive-shaped resonance appears at zero velocity class [Fig. 3(b)]. A closer
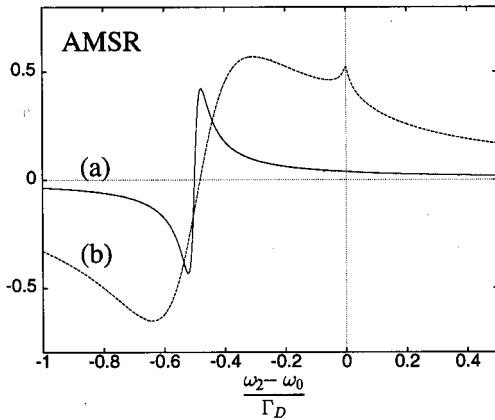
FIG. 3. Calculated AMSR Signal Eq. (6) for a red detuned pump laser ($\omega_1 - \omega_{ab} = -0.5 k_1 u$) for two different values of the saturation parameter: $S_{op} = 10$ (a) and $S_{op} = 100$ (b).

inspection shows that this resonance has the same line shape as the sub-Doppler singularity in usual linear SR signal from Eq. (1). This additional feature has the following origin: as the intensity of the pump laser is increased the resonant velocity class is saturated and one starts to saturate neighboring velocity classes. This is well known in transmission experiments, where it leads, among others, to the fact that a Doppler broadened line has a slower optical saturation behavior than the resonance line of an atom at rest (see, e.g., [22,23] and references therein). In transmission this does not lead to an extra resonance. In reflection, however, the discontinuity in the velocity dependence of the atomic response leads to an additional resonance. This additional structure is pronounced only for large saturation parameters $S_{op} \gtrsim 50$ [Fig. 3(b)]. Similar structures were predicted previously in a theoretical analysis describing a pump-probe scheme in nonlinear SR for a vapor of two-level atoms [16]. Following the assumption discussed above that departing atoms do not undergo VSOP one expects no resonances at all in the AMSR spectrum for a blue detuned pump laser.
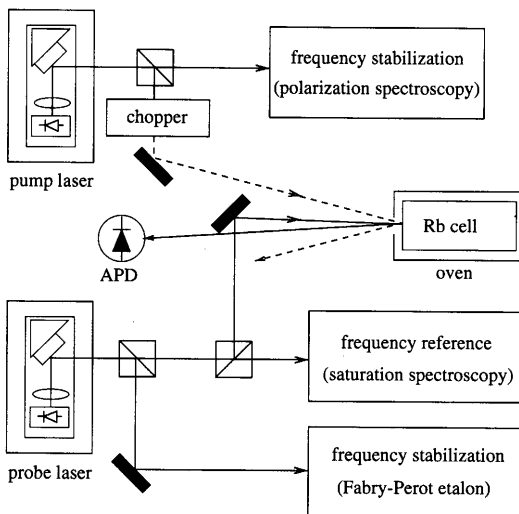

FIG. 4. Schematic experimental setup. The dashed line represents the amplitude modulated pump beam.

B. Experimental setup

Figure 4 shows a schematic diagram of the experimental arrangement. The light beams are produced by two grating-feedback stabilized diode lasers [26], and have a relative frequency jitter of 3 MHz as measured by recording their beat note. The beams have parallel linear polarizations and typical diameters of 2 mm. The amplitude of the pump beam is modulated at 2 kHz. Both beams are superposed and directed onto the window of a quartz cell at near-normal incidence. The evacuated cell contains natural Rb and is inside of an oven that allows one to control the Rb vapor pressure. The relative angle between the beams is on the order of $1-4$ mrad (corresponding to a residual Doppler width of $0.25-1$ MHz). The intensities can be independently controlled in the range of 50 μW-3 mW.

Long term frequency stabilization of both lasers is achieved by active feedback control. The pump beam is frequency locked to an auxiliary room-temperature vapor cell using polarization spectroscopy. This allows one to set the frequency of the pump laser to any hyperfine component of the two Rb isotopes as well as to the crossover resonances that occur halfway between any pair of these resonances. The probe laser, which is scanned in the experiments, is frequency locked to a transmission fringe of a confocal Fabry-Pérot resonator, in order to reduce acoustic frequency jitter. Scanning is done by ramping the separation of the Fabry-Pérot mirrors. Another auxiliary arrangement using the technique of amplitude-modulated saturated absorption (AMSA) in a room temperature Rb cell allows one to calibrate the frequency scale during the probe laser scans.

The variation of the intensity of the reflected probe beam is detected by an avalanche photodiode whose output is demodulated by a lock-in amplifier in phase with the amplitude modulation frequency. As the effective volume probed by the SR is very small ($\sim 10^{-6}$ cm^3), the cell containing the Rb vapor is heated to yield typical densities of $10^{13}-10^{14}$ cm^{-3}, in order to increase the signal-to-noise ratio.

To compare the line shapes of reflection and transmission signals the two beams can be sent copropagating through another Rb cell at room temperature (not shown in Fig. 4). The resonant variation of the transmitted light intensity of the probe beam is detected and demodulated by a lock-in amplifier.

C. Experimental results

Although the theoretical considerations presented above were restricted to a three-level system the obtained results can be easily extended to the multilevel structure of the Rb D_1 line used in our experiment. We recorded the reflected intensity of the weak probe beam as a function of probe detuning for various fixed frequencies of the amplitude modulated pump laser. Transmission and reflection spectra for three different, fixed pump laser frequencies are shown in Figs. 5, 6, and 7. In each spectrum the probe frequency is scanned over the hyperfine transitions $5S_{1/2}(F=2) \rightarrow 5P_{1/2}(F'=2,3)$ of the D_1 line of ^{85}Rb. The origin of the frequency axis is chosen to correspond to the $F=2 \rightarrow F'=3$ transition.
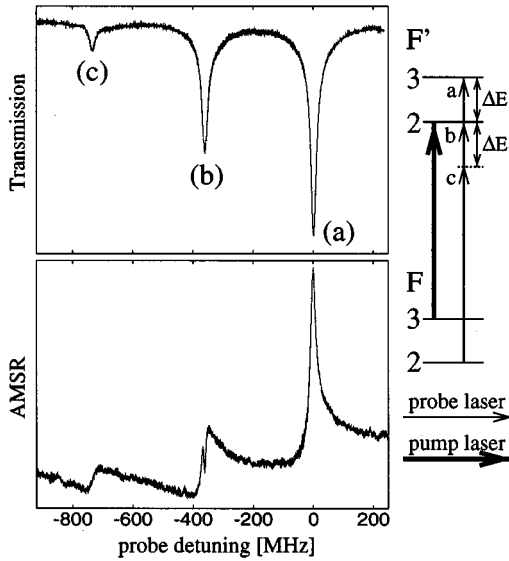
FIG. 5. Velocity selective optical pumping transmission and selective reflection spectra of the Rb D_1 line as function of the probe laser detuning from the $F=2 \rightarrow F'=3$ transition. The frequency of the pump laser was locked to the $F=3 \rightarrow F'=2$ hyperfine component.

1. Pump on $F=3 \rightarrow F'=2$ transition

The spectra in Fig. 5 have been recorded with the pump frequency locked to the $5S_{1/2}(F=3) \rightarrow 5P_{1/2}(F'=2)$ transition. In transmission one sees three resonances with power broadened Lorentzian line shapes. The origin of the lines can be understood as follows. The pump laser depletes the $F=3$ ground state and creates an excess of population in the $F=2$ ground state in a velocity selective manner. This transfer of population occurs on one hand for zero-velocity atoms
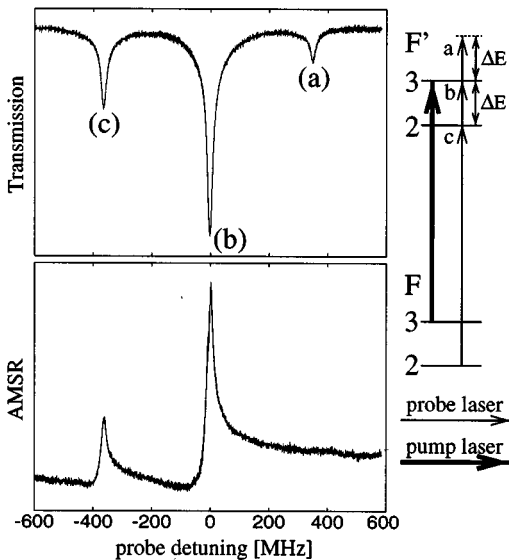

FIG. 6. Velocity selective optical pumping transmission and selective reflection spectra of the Rb D_1 line as a function of the probe laser detuning from the $F=2 \rightarrow F'=3$ transition. The frequency of the pump laser was locked to the $F=3 \rightarrow F'=3$ hyperfine component.
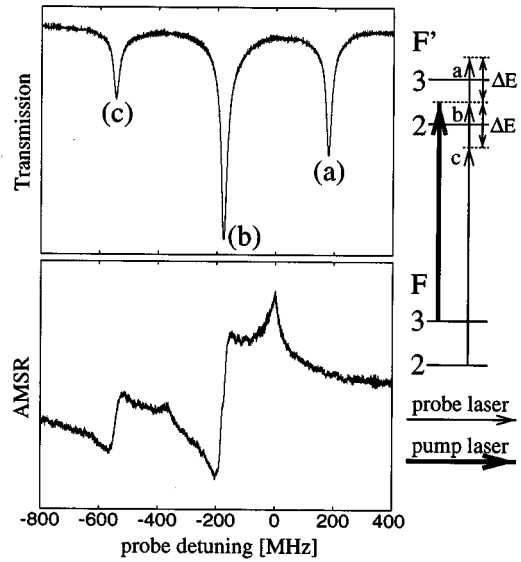

FIG. 7. Velocity selective optical pumping transmission and selective reflection spectra of the Rb D_1 line as function of the probe laser detuning from the $F=2 \rightarrow F'=3$ transition. The frequency of the pump laser was locked to the crossover resonance between the $F=3 \rightarrow F'=2$ and the $F=3 \rightarrow F'=3$ hyperfine components.

via the $F'=2$ excited state and on the other hand for atoms from a certain negative-velocity class via the $F'=3$ excited state. The negative-velocity atoms are Doppler shifted into resonance when their velocity v is given by $k_1 v = -\Delta \omega_{\text{hf}}$, where $\hbar \Delta \omega_{\text{hf}} = \Delta E$ is the hyperfine splitting of the excited state. The probe laser probes the excess of population in the $F=2$ ground state in a resonant manner and the negative signal amplitudes reflect an increased probe absorption. In this way resonance (a) comes from zero-velocity atoms, resonances (c) from negative-velocity atoms, and resonance (b) from both velocity classes.

The reflection spectrum looks much more complicated and shows a variety of different line shapes. All resonances can be understood and theoretically reproduced by the model of incoherent optical pumping processes developed above. The resonance (a) comes from zero-velocity atoms for which the $F=3 \rightarrow F'=2$ transition is resonant with the pump laser and the $F=2 \rightarrow F'=3$ transition is resonant with the probe laser. The observed asymmetric absorptive line shape agrees with the one predicted by our model for a resonant pump laser [Fig. 2(b)]. The small dispersively shaped resonance at -720 MHz [line (c) in Fig. 5] is due to negative-velocity atoms that interact with the pump laser via the $F=3 \rightarrow F'=3$ transition and with the probe laser via the $F=2 \rightarrow F'=2$ transition. The line shape corresponds to the one calculated for a nonresonant pump laser (Fig. 3). Atoms from both the zero-velocity class (pump laser resonant with $F=3 \rightarrow F'=2$ and probe laser resonant with $F=2 \rightarrow F'=2$) and the resonant negative-velocity class (pump laser resonant with $F=3 \rightarrow F'=3$ and probe laser resonant with $F=2 \rightarrow F'=3$) give rise to the resonance (b) from Fig. 5. The complex line shape observed is just the sum of the two line shapes with different symmetries. The zero-velocity atoms, again lead to an absorptively shaped resonance, whereas the negative velocity atoms give rise to a dispersion.

The central resonance [line (b)] is also the one that fulfills the resonance criteria for a Λ-type transition (i.e., both lasers coupled to a common upper state). The dip in the line shape may therefore easily be misinterpreted in terms of a dark resonance. We stress, however, that in this case the structure can be fully explained as the superposition of two line shapes coming from *incoherent* processes. We checked this experimentally by verifying that the structure cannot be destroyed by a magnetic field. Ground state coherences are known to be extremely sensitive to even small magnetic perturbations. The insensitivity of the resonance to magnetic fields is another proof of its incoherent nature.

2. Pump on $F=3 \rightarrow F'=3$ transition

The spectra in Fig. 6 were recorded with the pump frequency locked to the $5S_{1/2}(F=3) \rightarrow 5P_{1/2}(F'=3)$ hyperfine component. In this case the population transfer occurs via the $F'=3$ exited state for atoms with zero velocity and via the $F'=2$ state for a certain velocity class of departing atoms. The transmission spectrum shows again three Lorentzian shaped lines, where line (a) comes from atoms with positive velocities, line (c) from atoms with zero velocity, and line (b) again from atoms of both velocity classes. After the previous discussion the reflection spectrum is easily understood. Lines (b) and (c) have the typical shapes induced by a *resonant pump* laser. Note that if there was no difference in the behavior of atoms with negative and positive velocities one would expect line (b) to have the same complex structure as line (b) in Fig. 5. However, line (b) has merely the typical profile expected from zero-velocity atoms; the contribution from departing atoms is absent. The latter fact is even more clearly evidenced by the complete absence of line (a) in the reflection spectrum. Only departing atoms would contribute to this line. This is direct experimental evidence that in selective reflection experiment departing atoms (positive velocities) cannot be optically pumped, thus justifying the theoretical assumption made above.

3. Pump on crossover between the $F=3 \rightarrow F'=2$ and the $F=3 \rightarrow F'=3$ transitions

Finally, the spectra shown in Fig. 7 were recorded with the pump frequency locked to the crossover resonance between the hyperfine transitions $F=3 \rightarrow F'=2$ and $F=3 \rightarrow F'=3$. In this case positive velocity atoms are pumped via the $F'=2$ excited state and negative velocity atoms via the $F'=3$ state, while no zero-velocity atoms are pumped. While the transmission spectrum shows the usual three lines, four distinct structures appear in the reflection spectrum. The resonance (a) at $+180$ MHz is again missing since atoms with positive velocities are not optically pumped. In addition to the two dispersive VSOP signals (b) and (c), which are due to atoms with negative velocities one can observe two additional resonances at the positions of the two single photon resonances of the probe transitions $F=2 \rightarrow 2$ (at -362 MHz) and $F=2 \rightarrow 3$ (at 0 MHz). These resonances do not show up in the transmission spectrum. The line shape of these resonances looks similar to the line shape of the linear selective reflection but one has to keep in mind that these resonances are correlated with the presence of the pump laser (lock-in detection).
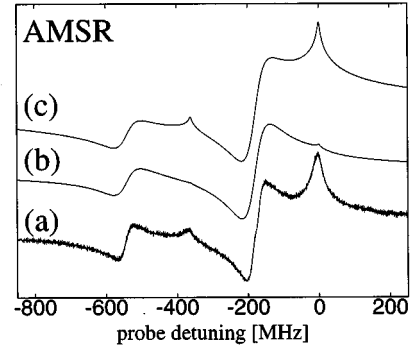

FIG. 8. AMSR signal as a function of the probe laser detuning with respect to the $F=2 \rightarrow F'=3$ transition. The frequency of the pump laser was locked to the crossover resonance between the $F=3 \rightarrow F'=2$ and the $F=3 \rightarrow F'=3$ transitions. Comparison between the experimental spectrum (a) and two calculated spectra (b) and (c). In spectrum (c) a 30% survival rate of the optically pumped ground-state populations has been assumed.

The theoretically predicted small additional structure at zero detuning [see Fig. 3(b)] does not fully account for the observed lines as the amplitudes of the experimental peaks are much larger than the predicted ones. A possible explanation for these resonances is an incomplete rethermalization of the hyperfine ground-state populations during the collision of the atoms with the wall. Previous experiments done with sodium atoms in a glass cell [27] have shown that a certain fraction of optically pumped atoms remain in the same hyperfine ground state even after a collision with a wall. If we assume that this also holds for Rb atoms colliding with the cell window, but that the velocity of the departing atoms is random, i.e., not correlated to their initial velocity, then the red detuned pump laser that is velocity selective for the arriving atoms acts like a broadband velocity independent pump for the departing atoms. From the amplitudes of these extra resonances relative to the VSOP signal amplitude one can therefore determine the fraction of departing atoms that have remained in their initial hyperfine state after a single wall collision. A coarse analysis yields a value between 30% and 50%. This is in agreement with a recent measurement done on sodium atoms in a buffer gas cell [28]. However, the method presented here does require less theoretical assumptions to obtain a quantitative measure of the depolarization properties of the glass surface.

We have simulated the whole experimental spectrum for a red detuned pump field. Spectrum 8(a) reproduces the experimental spectrum of Fig. 7. Spectrum 8(b) is obtained from the regular VSOP spectrum discussed in Sec. III A. In Fig. 8(c) we have added linear selective reflection signals by assuming a 30% fraction of departing atoms that have survived the wall collision in their initial hyperfine state. There is a remarkably good agreement between experiment [Fig. 8(a)] and theory [Fig. 8(c)]. However, for a full quantitative theory of this effect, a more detailed investigation has to be done where one also has to take into account other possible effects such as velocity changing collisions among the atoms. In a time resolved experiment an interesting application of this phenomenon would be to measure the delay between the optical pumping of the arriving atoms and the appearance of the peak from the departing atoms thus determing in the time of residence of the atoms on the glass surface.
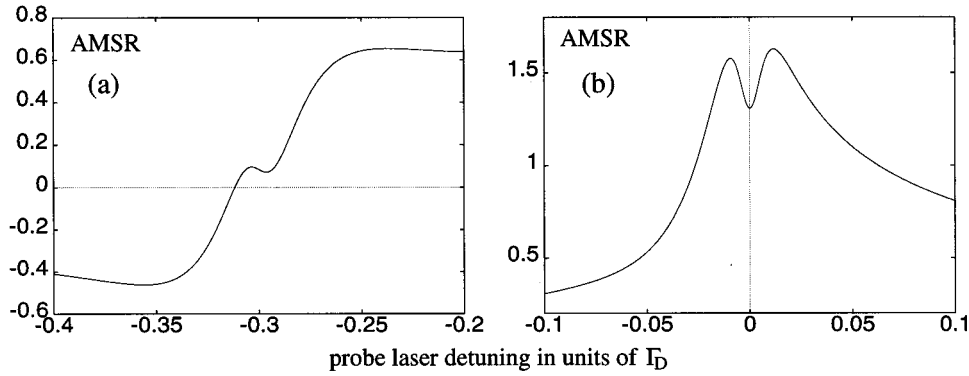
FIG. 9. Calculated AMSR signal [Eq. (8)], (a) for a red detuned pump laser ($\omega_1 - \omega_{ab} = -0.3ku$), and (b) for a resonant pump laser ($\omega_1 - \omega_{ab} = 0$). Note the dark resonance is an additional feature superimposed on the large background due to VSOP.

IV. DARK RESONANCES IN SR SPECTROSCOPY

A. Theory

One of the main objectives of this project was the observation of coherent effects in selective reflection. In order to include coherences in our theoretical approach we apply the density matrix formalism to the atomic system. As before we will consider the Λ system from Fig. 1 and use the indices 1 and 2 to refer to the pump and probe fields, respectively. Both light fields have the same linear polarization. In addition we will consider a relaxation rate Γ_{coh} for the coherences between the ground-state levels, which in general differs from the population relaxation rate Γ. In our experiments this relaxation is dominated by the finite transit time but it is also sensitive to relative phase and frequency jitter of the two laser fields. We neglect longitudinal atomic relaxation by collisions and also the magnetic substructure of each level. We use the results of a previous calculation by Hänsch and Toschek [Eq. (25) in [21]] for a gas of three-level atoms interacting with two copropagating laser fields of different frequencies. Their result gives the stationary solution for the optical coherence ρ_{bc} in the linear approximation for both pump and probe field $\Omega_2 \ll \Omega_1 \ll \gamma$, where $\Omega_{1,2}$ are the Rabi frequencies of the pump and the probe field, respectively. The off-diagonal element ρ_{bc} describes the oscillating polarization on the probe transition, which gives the resonant variation of the reflectivity of the probe beam:

$$\rho_{bc} = (\rho_{bb} - \rho_{cc})\frac{\Omega_2}{\Delta_{bc}} + (\rho_{bb} - \rho_{aa})\frac{\Omega_2|\Omega_1|^2}{\Delta_{ab}\Delta_{bc}\Delta_{ac}}$$
$$+ (\rho_{bb} - \rho_{cc})\frac{\Omega_2|\Omega_1|^2}{\Delta_{bc}^2\Delta_{ac}}, \tag{7}$$

with

$$\Delta_{ab} = \omega_{ab} + \mathbf{k}_1 \cdot \mathbf{v} - \omega_1 + i\gamma/2,$$

$$\Delta_{bc} = -\omega_{bc} - \mathbf{k}_2 \cdot \mathbf{v} + \omega_2 + i\gamma/2,$$

$$\Delta_{ac} = (\omega_2 - \omega_{bc}) - (\omega_1 - \omega_{ab}) + (\mathbf{k}_1 - \mathbf{k}_2) \cdot \mathbf{v} + i\Gamma_{\text{coh}},$$

where ρ_{ii} are the stationary state populations. In the limit where $\Gamma \ll \gamma$ these populations are $\rho_{bb} = 0$, $\rho_{aa} = \frac{1}{2}(1 - L)$, $\rho_{cc} = \frac{1}{2}(1 + L)$, where L is the line shape of the hole given by Eq. (5). In our experiment the levels a and c belong to the same fine-structure level so we will take $\mathbf{k}_1 = \mathbf{k}_2$.

The SR signal is proportional to the real part of the off-diagonal element ρ_{bc}. After subtracting the linear contribution to the signal we find the amplitude modulated selective reflection coefficient of the probe field

$$I_{\text{AMSR}} \propto \int_{-\infty}^{0} dv\, W(v)\,\text{Re}\left\{ \underbrace{\frac{L}{\Delta_{bc}}}_{\text{VSOP}} + \underbrace{\frac{(1-L)|\Omega_1|^2}{\Delta_{ab}\Delta_{bc}\Delta_{ac}} + \frac{(1+L)|\Omega_1|^2}{\Delta_{bc}^2\Delta_{ac}}}_{\text{coherent effects}} \right\}. \tag{8}$$

Note that the first term in brackets describes the incoherent VSOP signal discussed above [Eq. (6)]. The second and third terms describe the coherent effects and lead to narrow structures in the AMSR signal, which can be identified as dark resonances.

In Fig. 9 the total AMSR signal as given by Eq. (8) is shown. In Fig. 9(a) the frequency of the pump laser is *red*

detuned by $-0.3ku$ from the atomic resonance, which corresponds approximately to an experimental detuning of -120 MHz. The VSOP term leads to the large dispersion-shaped background known from Fig. 3. The coherent terms give rise to a symmetrical dispersive signal superimposed on the VSOP signal with opposite sign. The dark resonance is centered at $-0.3ku$ and has a linewidth on the order of
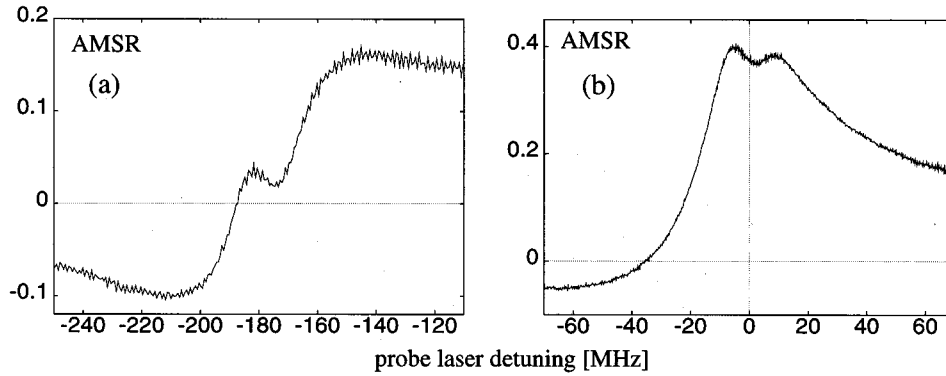
FIG. 10. Experimental observation of dark resonances in SR spectroscopy. In (a) the frequency of the pump laser was red detuned by -181 MHz from the $F=3 \rightarrow F'=3$ transition, and in (b) the pump laser was resonant with the transition.

Γ_{coh}. The total AMSR signal calculated for a *resonant* pump laser is shown in Fig. 9(b). The VSOP term is again responsible for the large background structure (Fig. 2) on which the dark resonance is superimposed. The dark resonance is an absorptively shaped resonance of width Γ_{coh} and of opposite sign than the VSOP signal.

B. Experimental results

A close look at the large dispersive structure in the center of Fig. 7, which was recorded with small probe and large pump intensities, reveals a small structure in the center of the line. If one increases the intensity of the probe beam the amplitude of the VSOP signal decreases because of repumping by the probe laser while the amplitude of the dark resonance increases. In Fig. 10 we present two spectra taken with equal laser intensities ($I_1 = I_2 = 3$ mW). First, the frequency of the pump laser was red detuned by -181 MHz with respect to the $F=3 \rightarrow 3$ transition frequency [Fig. 10(a)], and second the pump laser was resonant with the transition [Fig. 10(b)].

The large symmetric dispersion in the spectrum (a) and the large absorptive line in the spectrum (b) are the VSOP signals discussed in the previous section. Superimposed on these lines one can clearly observe the dark resonances. The following arguments support the hypothesis that the observed changes in the VSOP signal are indeed due to coherence effects (dark resonance): (i) The resonances appear exactly at the position of the Raman resonance condition $\omega_1 - \omega_2 = \omega_{ac}$. (ii) The application of a transverse magnetic field destroys the dark resonance without affecting the VSOP signals. (iii) The line shape and the sign of the dark resonance are in agreement with the theoretical predictions (Fig. 9).

For the red detuned pump laser the agreement between the theoretical prediction and the experimental spectrum is fairly good. In the resonant case the theoretical and experimental line shapes agree less well. A possible explanation for this fact is the omission in the theoretical model of long-range interactions between the atoms and the cell window. The effect of these interactions is especially pronounced for slow atoms, which spend a long time near the surface. But

these slow atoms from the zero velocity class give the main contribution to the total AMSR signal for a resonant pump laser. With a blue detuned pump we did not observe any dark resonances, although a theoretical calculation by Nienhuis and Schuller [18] does predict a narrow resonance in that case.

The measured linewidth of the dark resonance is about 20 MHz which is 3 times smaller than the saturation broadened linewidth of the VSOP signal (60 MHz) but still larger than the natural linewidth (5 MHz) of the transition. The ultimate linewidth depends only on the relaxation rate of the ground-state coherences, which may lead to subnatural resonances. We attribute the fact that we did not observe a subnatural linewidth to the joint effects of time-of-flight, high laser intensities, residual magnetic fields, and phase jitter of the two lasers.

V. CONCLUSION

In this paper we have presented an experimental observation of dark resonances in selective reflection spectroscopy. For a proper identification of the coherent effects a detailed study of velocity selective optical pumping has been performed. A simple theoretical model was used to model the spectra.

One of the main results is the direct experimental proof that atoms departing from the surface are not optically pumped and do not contribute to the VSOP signal. The line shape of the VSOP signal has a complex frequency dependence, which can be fully explained by the different behavior of atoms arriving to the surface and atoms departing from the surface. In the experiments additional resonances have been observed, which cannot be explained by VSOP, but which are probably due to an incomplete rethermalization of the hyperfine ground-state populations during the wall collision. The effect of velocity changing collisions between the atoms has not been considered but will be the subject of future investigations.

We have furthermore performed an experimental study of dark resonances in reflection spectroscopy. The line shapes of the observed dark resonances agree with the calculated ones. For blue detuned lasers no dark resonances were ob-

served, which is a further proof that no coherences between ground states can be built up for departing atoms. The dark resonance for zero detuning is broadened and its amplitude is less than the calculated one. This also is a hint that the long-range van der Waals interaction between the atoms and the surface may effect the relaxation time of ground-state coherences.

---

[1] R. W. Wood, Philos. Mag. **18**, 187 (1909).

[2] J. L. Cojan, Ann. Phys. (France) **9**, 385 (1954).

[3] J. P. Woerdman and M. F. H. Schuurmans, Opt. Commun. **14**, 248 (1975).

[4] For a review see, e.g., M. Ducloy, in *Quantum Optics VI*, Proceedings of the Sixth International Symposium on Quantum Optics, Rotorua, New Zealand, edited by D. F. Walls and J. D. Harvey (Springer, Berlin, 1994).

[5] A. M. Akul'shin, V. L. Velichansky, A. S. Zibrov, V. V. Nikitin, V. A. Sautenkov, E. K. Yurkin, and N. V. Senkov, Pis'ma Zh. Éksp. Teor. Fiz. **36**, 247 (1982) [JETP Lett. **36**, 303 (1982)].

[6] V. Vuletic, V. A. Sautenkov, C. Zimmermann, and T. W. Hänsch, Opt. Commun. **99**, 185 (1993).

[7] N. Papageorgiou, M. Fichet, V. Sautenkov, D. Bloch, and M. Ducloy, Laser Phys. **4**, 392 (1994).

[8] M. Oria, M. Chevrollier, D. Bloch, M. Fichet, and M. Ducloy, Europhys. Lett. **14**, 527 (1991).

[9] M. Chevrollier, D. Bloch, G. Rahmat, and M. Ducloy, Opt. Lett. **16**, 23 (1991).

[10] N. Papageorgiou, A. Weis, V. A. Sautenkov, D. Bloch, and M. Ducloy, Appl. Phys. B **59**, 123 (1994).

[11] G. Stanzel, Z. Phys. **270**, 361 (1974).

[12] G. W. Series, Proc. Phys. Soc. **91**, 432 (1967).

[13] A. Weis, V. A. Sautenkov, and T. W. Hänsch, Phys. Rev. A **45**, 11 (1992).

[14] A. Weis, V. A. Sautenkov, and T. W. Hänsch, J. Phys. II (France) **3**, 263 (1993).

[15] T. A. Vartanyan, Sov. Phys. Zh. Éksp. Teor. Fiz. **41**, 297 (1985) [JETP **41**, 364 (1985)].

[16] F. Schuller, G. Nienhuis, and M. Ducloy Phys. Rev. A **43**, 443 (1991).

[17] F. Schuller, O. Gorceix, and M. Ducloy, Phys. Rev. A **47**, 1 (1993).

[18] G. Nienhuis and F. Schuller, Phys. Rev. A **50**, 2 (1994).

[19] N. Papageorgiou, Ph.D. thesis, Université Paris-13, 1994 (unpublished).

[20] A. Amy-Klein, S. Saltiel, O. A. Rabi, and M. Ducloy, Phys. Rev. A **52**, 3101 (1995).

[21] T. W. Hänsch and P. Toschek, Z. Phys. **236**, 213 (1970).

[22] M. S. Feld and A. Javan, Phys. Rev. Lett. **177**, 540 (1969).

[23] V. S. Letokhov and V. Chebotayev, in *High Resolution Laser Spectroscopy*, Topics in Applied Physics Vol. 13, edited by K. Shimoda (Springer, Berlin, 1976).

[24] M. Ducloy and M. Fichet, J. Phys. (France) **1**, 1429 (1991).

[25] M. F. H. Schuurmanns, Contemp. Phys. **21**, 463 (1980).

[26] L. Ricci, M. Weidemüller, T. Esslinger, A. Hemmerich, C. Zimmermann, V. Vuletic, W. König, and T. W. Hänsch, Opt. Commun. **117**, 541 (1995).

[27] J. E. M. Haverkort, R. W. M. Hoogeveen, and J. P. Woerdman, Opt. Commun. **61**, 109 (1987).

[28] S. Grafström and D. Suter, Opt. Lett. **20**, 2134 (1995).